HHS Public Access

Author manuscript

*Clin Cancer Res*. Author manuscript; available in PMC 2023 April 14.

Published in final edited form as:

*Clin Cancer Res*. 2022 October 14; 28(20): 4479–4493. doi:10.1158/1078-0432.CCR-22-1627.

# Combined TRIP13 and Aurora kinase inhibition induces apoptosis in human papillomavirus–driven cancers

**Soma Ghosh**[1], **Tuhina Mazumdar**[1], **Wei Xu**[1,†], **Reid T. Powell**[2], **Clifford Stephan**[2], **Li Shen**[3], **Pooja A. Shah**[1], **Curtis R. Pickering**[4,6], **Jeffery N. Myers**[4,6], **Jing Wang**[3,6], **Mitchell J. Frederick**[5], **Faye M. Johnson**[4,6,*]

[1]Department of Thoracic/Head & Neck Medical Oncology, The University of Texas MD Anderson Cancer Center, Houston, Texas.

[2]Center for Translational Cancer Research, Institute of Biosciences and Technology, Texas A&M College of Medicine, Houston, Texas.

[3]Department of Bioinformatics and Computational Biology, The University of Texas MD Anderson Cancer Center, Houston, Texas.

[4]Department of Head and Neck Surgery, The University of Texas MD Anderson Cancer Center, Houston, Texas.

[5]Department of Otolaryngology, Baylor College of Medicine, Houston, TX 77030, USA

[6]The University of Texas Graduate School of Biomedical Sciences, Houston, Texas.

## Abstract

**Purpose:** Human papillomavirus (HPV) causes >5% of cancers but no therapies uniquely target HPV-driven cancers.

**Experimental Design:** We tested the cytotoxic effect of 864 drugs in 16 HPV-positive and 17 HPV-negative human squamous cancer cell lines. We confirmed apoptosis *in vitro* and *in vivo* using patient derived xenografts. Mitotic pathway components were manipulated with drugs, knockdown, and overexpression.

**Results:** Aurora kinase inhibitors were more effective *in vitro* and *in vivo* in HPV-positive than in HPV-negative models. We hypothesized that the mechanism of sensitivity involves

[*]**Corresponding author**. Faye M. Johnson, M.D., PhD., Faculty, Graduate School of Biomedical Sciences; Professor, Thoracic, Head and Neck Medical Oncology, University of Texas, M.D. Anderson Cancer Center, 1515 Holcombe, Box 432, Houston, TX 77030, phone 713-792-6363, fax 713-792-1220, fmjohns@mdanderson.org.

[†]Present address: Key Laboratory of Geriatrics of Jiangsu Province, Department of Geriatrics, The First Affiliated Hospital of Nanjing Medical University, Nanjing, Jiangsu, PR China.

Author contributions:

SG, TM, RP, CS, and FMJ designed the research.
SG, TM, PS, and WX performed the experiments
FMJ conceived and oversaw the project
LS, JW, RP, CS, CP, and MF performed the bioinformatic analysis
SG, TM, and FMJ analyzed the data
SG and FMJ wrote the paper
JM provided data and critically edited the manuscript

**Competing interests:** Faye M. Johnson has received research funding from The Takeda Pharmaceutical Company, Viracta Therapeutics, and Trovagene. All other authors declare no potential conflicts of interest.

retinoblastoma (RB) expression because the viral oncoprotein E7 leads to RB protein degradation, and basal RB protein expression correlates with Aurora inhibition–induced apoptosis. Manipulating RB directly, or by inducing E7 expression, altered cells' sensitivity to Aurora kinase inhibitors. RB affects expression of the mitotic checkpoint genes *MAD2L1* and *BUB1B* which we found to be highly expressed in HPV-positive patient tumors. Knockdown of *MAD2L1* or *BUB1B* reduced Aurora kinase inhibition-induced apoptosis, whereas depletion of the MAD2L1 regulator TRIP13 enhanced it. TRIP13 is a potentially druggable AAA-ATPase. Combining Aurora kinase inhibition with TRIP13 depletion led to extensive apoptosis in HPV-positive cancer cells but not in HPV-negative cancer cells.

**Conclusions:** Our data support a model in which HPV-positive cancer cells maintain a balance of MAD2L1 and TRIP13 to allow mitotic exit and survival in the absence of RB. Because it does not affect cells with intact RB function, this novel combination may have a wide therapeutic window, enabling the effective treatment of RB-deficient cancers.

### Keywords

Human papillomavirus; head and neck squamous cell carcinoma; Aurora kinase; mitotic checkpoint; TRIP13

## INTRODUCTION

Each year, there are 694,000 new cases of human papillomavirus (HPV)-driven cancers worldwide (1). HPV causes more than 5% of cancers (2), including head and neck squamous cell carcinoma (HNSCC) and squamous cancers of the cervix, anus, penis, and vulva (3). HPV-driven cervical cancer is the leading cause of cancer death in women in the developing world, and the incidence of HPV-positive HNSCC in the developed world is rising (2,4). The treatment of HPV-positive HNSCC, which usually presents as locally advanced disease, involves a combination of cisplatin chemotherapy and radiotherapy and results in decades-long, chronic, therapy-related adverse effects, including difficulty swallowing, dry mouth, feeding tube dependence, and aspiration pneumonia (5). Consequently, de-intensified therapies and new therapies focusing on druggable targets for HPV-associated HNSCC are being widely investigated with the aim of reducing mortality and treatment-associated morbidity (6).

Several independent investigators have defined the genetic landscape of HPV-positive HNSCC, which is distinct from HPV-negative HNSCC and have identified potential pathways controlling cell cycle dysregulation and constitutive cell proliferation (7,8). Another distinct molecular feature of HPV-positive cancers is that they express the viral oncoproteins E6 and E7, which lead to p53 and retinoblastoma (Rb) protein degradation and thus disrupts cell cycle regulation and provides a mechanism for tumorigenesis (9). However, none of these findings has translated into improved therapies.

Although HPV-positive tumors are molecularly distinct from HPV-negative tumors, their treatments are identical. In the current study, we sought to identify HPV status–selective therapies using a high-throughput drug screen (HTDS) with diverse drugs. We focused on identifying drugs that caused cell death and identified Aurora kinase inhibitors as the

only drug class that was consistently more effective against HPV-positive cancers than HPV-negative cancers. We hypothesized that Rb-deficient, HPV-positive cells that overexpress the mitotic checkpoint gene Mad2 (*MAD2L1*) rely on both TRIP13 and Aurora kinase activity to maintain mitotic fidelity, such that the combined inhibition of TRIP13 and Aurora kinase activity can lead to irreversible mitotic arrest, DNA damage, and apoptosis. Therefore, in this study, we also investigated the roles of Rb, Mad2, and TRIP13 in Aurora kinase inhibition–induced apoptosis in HPV-positive cancers. Our results demonstrate that Rb-deficient cancers are sensitive to Aurora kinase inhibition because of an imbalance between Mad2 and TRIP13. To the best of our knowledge, this is the first study to demonstrate that TRIP13 depletion in combination with Aurora kinase inhibition leads to significantly more apoptosis than does single pathway inhibition selectively in HPV-positive cancers. This finding may lead to the development of novel therapies for the management of Rb-deficient cancers.

## MATERIALS AND METHODS

### Cells lines and reagents

HNSCC and cervical squamous carcinoma cell lines were obtained, maintained, and profiled as described previously (10). Tests performed included RPPA (11,12), RNA-seq (13), HPV integration (13), and whole-exome sequencing (14). RPPA was performed on 28 cell lines in the HTDS in a single batch to avoid batch effects (11,12). No RPPA data were available for HN31, PCI15B, UMSCC1, UMSCC22A, or UMSCC25. All cell lines were genotyped using short tandem repeat analysis, and all were mycoplasma-free at the time of testing as determined using a mycoplasma detection kit (Lonza, Walkersville, MD). All drugs, except those used in the HTDS, were purchased from Selleck Chemicals (Houston, TX) and prepared as 10 mmol/L stock solutions in DMSO. Antibodies are listed in Table S1.

### Immunoblotting

Western blot analysis was performed as described previously (15). In brief, cells were lysed with ice-cold lysis buffer, and the lysates were centrifuged at 20,000 × g for 10 minutes at 4 °C. Cell lysates containing equal amounts of protein were resolved using sodium dodecyl sulfate–polyacrylamide gel electrophoresis, transferred to nitrocellulose membranes, and incubated with different primary antibodies. Protein expression was detected using a horseradish peroxidase–conjugated secondary antibody (Bio-Rad, Hercules, CA) and electrochemiluminescence reagent (Amersham Biosciences, Pittsburg, PA). For the quantification of protein expression, the band intensities were measured using ImageJ, RRID:SCR_003070 (National Institutes of Health, Bethesda, MD) (16) and normalized first to β actin and then to its respective positive control (expression in HN31, UMSCC4, or C33A, as noted in the figures).

### Apoptosis, cell cycle, and senescence assays

To measure apoptosis, we performed TUNEL staining with an APO-BRDU Kit (BD Biosciences, San Jose, CA) and annexin V/propidium iodide staining with an FITC Annexin V Apoptosis Detection Kit PE (eBioscience, San Diego, CA) as described previously (12). For the cell cycle analysis, cells were harvested, fixed, incorporated

with bromodeoxyuridine (BrdU), and stained with 7-aminoactinomycin D using a BrdU Flow Kit (BD Biosciences, San Jose, CA). Data were acquired with a 3-laser, 10-color Gallios flow cytometer (Beckman Coulter, Brea, CA) and analyzed using Kaluza software, RRID:SCR_016182 (Beckman Coulter, Brea, CA). Assays were performed in triplicate, and each test was completed twice on different days. To measure senescence, we stained cells using the CellEvent Senescence Green Detection Kit (Thermofisher Scientific, Waltham, MA). Briefly, after drug treatment, cells were incubated with Senescence Green Probe, a fluorescence-based reagent that contains 2 galactoside moieties that make it specific to β-galactosidase. The enzyme-cleaved product is retained within the cell and it emits a fluorogenic signal that we measured at 490/514 nm using a flow cytometer.

### siRNA transfection

siRNA molecules (5 nmol/L, GE Dharmacon, Lafayette, CO and 5 nmol/L, Santa Cruz Biotechnology, Inc., Dallas, Tx) targeting *E7*, *TRIP13*, *MAD2L1*, and *BUB1B* or scrambled controls were transfected into cells using lipofectamine RNAi Max (ThermoFisher, Waltham, MA) in Opti-MEM (Invitrogen, Waltham, MA) according to the manufacturers' standard protocols. Cells were transfected with siRNA for 24 hours prior to the initiation of drug treatment.

### Generation of stable cells using lentiviral infection

The lentiviral-based shRNA (GIPZ plasmid) used to knock down human *RB1* expression was purchased from Horizon Discovery (Waterbeach, United Kingdom). On the basis of the knockdown efficiency of Rb1 protein expression in 3 HPV-negative cell lines (HN31, UMSCC4, and MDA88 6LN), we selected 3 shRb1clones (#2, #4, and #6) for this study. These were the clones with the greatest reductions in Rb1 protein expression. The mature antisense sequences were as follows: 5′-TAAAGATGTATCCTATATC-3′ (shRb1 #2), 5′-TTAACTGAAATGAAATCAC-3′ (shRb1 #4), and 5′-TAAGTTCACATGTCCTTTC-3′ (shRb1 #6). To generate lentivirus-expressing shRNA for *RB1*, we transfected HEK 293T cells with GIPZ-non-silence (for the vector control virus) and GIPZ-shRB1 with jetPEI transfection reagent (RRID:CVCL_0063). The medium was changed 24 hours after transfection and then collected every 48 hours thereafter. The collected lentivirus-containing medium was centrifuged and then filtered (0.45 μM). Cells cells were seeded at 50% confluence 12 hours before infection, and the medium was replaced with a medium containing lentivirus. After 24 hours, the medium was replaced and the infected cells were selected with 2.5 μg/mL puromycin (Sigma-Aldrich, St. Louis, MO).

### *In vivo* tumor growth study

The *in vivo* tumor growth study was performed in accordance with the Guide for the Care and Use of Laboratory Animals of the National Institutes of Health and approved by MD Anderson's Institutional Animal Care and Use Committee. The PDX models were generated as described previously (17) and subjected to qPCR as described to determine the HPV type (18,19). Briefly, tumor tissue was cut into small fragments (5–6 mm) and implanted subcutaneously into the flanks of nude mice. The skin incisions were closed with skin clips that were removed after 10 to 15 days. Once tumors reached an average of 150 to 300 $mm^3$, the mice were randomized into either vehicle group or alisertib group.

Alisertib (Takeda Pharmaceuticals, Lexington, MA; 10 mg/kg in 10% β-cyclodextrin) was administered via oral gavage once daily on a weekly schedule of 6 days on and 1 day off. Tumors were monitored daily, and tumor volume (length × width$^2$ × 0.5) was evaluated twice per week with digital calipers. Mice were euthanized when tumors reached 2000 mm$^3$. The endpoint for the survival studies was the tumor burden. Survival was measured using the Kaplan-Meier method (20). Survival curve analysis was performed with GraphPad Prism software version 9 (RRID:SCR_002798).

### Genomic data from TCGA cohorts.

Files containing raw RSEM count data from the TCGA RNA-seq datasets that were previously harmonized computationally and mapped through the Toil open source calling pipeline (21) were downloaded from Amazon web services (AWS) S3 as previously described. RSEM counts were normalized to get upper quartile FPKM values (FPKM-UQ) with an in-house script in R studio. Essentially, non-protein coding RNAs were removed using annotations from Ensembl, which left 19,345 genes. The 75$^{th}$ percentile RSEM value (excluding zeros) for each TCGA sample was calculated and used to derive FPKM-UQ values. For most statistical analyses, the log 2 (FPKM-UQ +0.01) transformation was applied.

A total of 517 RNA-seq samples from HNSCC tumors were acquired (7) using original TCGA marker approach. Detection of HPV infection and HPV integration and measurement of HPV gene expression in TCGA data sets were performed by applying the VirusSeq pipeline RRID:SCR_005206 (22). Tumor HPV status was established by considering an empirical cutoff of 1000 read counts mapped against the viral genome (23).

### Statistical analyses

We computed the concordance correlation coefficient to assess the reproducibility of the normalized growth rates of the 2 replicates. To determine whether drugs of the same target class cluster together because of similar drug potency, we performed unsupervised drug clustering based on AOC_LD values. In the clustering analysis, we observed 6 distinct drug clusters based on the clustering trees. We then applied chi-square test to compare drug classification and the cluster membership. We also applied the Fisher exact test to compare mutations status (wild-type and mutant) and drugs' response data (sensitive and resistant). In these analyses, $p \leq 0.05$ was considered statistically significant.

To identify protein markers, we compared RPPA protein expression levels between drug-sensitive and -resistant groups using 2-sample *t*-tests. We used the Benjamini-Hochberg method to adjust for multiple hypothesis testing. We used an appropriate false discovery rate *q* value to identify protein markers significantly associated with drug-sensitive or -resistant groups. All statistical and bioinformatical analyses were performed using R (version 3.6.0).

### Data Availability Statement

The data generated in this study are available within the article and its Supplementary Data files. For any data used in this study that is not included in the paper or supplementary files can be made available upon request from the corresponding author.

# RESULTS

## Landscape of drugs that cause cell death in squamous carcinoma

We tested the effects of 864 unique drugs from 51 classes (Table S2) in 16 HPV-positive and 17 HPV-negative HNSCC and cervical squamous cancer cell lines (Table S3) that we characterized previously (13). Drugs without a well-defined target or with unique targets (i.e., targets not shared with other drugs in the screen) were categorized as "other." As with our previous HTDS (12), the quality control metrics showed that the data were reproducible (Supplementary Fig. S1).

Because traditional methods of measuring drug sensitivity (e.g., calculating $IC_{50}$ values) can be confounded by the number of cell divisions during the course of an assay, we adapted an alternative method whose results are independent of the cell division rate (24). In this method, the area-over-the-curve lethal dose (AOC_LD) value is 0 when a drug does not kill cancer cells at any concentration and greater than 0 when cell death occurs; it has a maximum value of 1 (Supplementary Fig. S2A).

About half the drugs tested (n = 425; 49%) had AOC_LD values of 0, and thus were ineffective, in all cell lines. The rest of the drugs (n = 439; 51%) were potentially effective, as they led to cell death in at least one cell line. To determine if certain classes of drugs were more or less likely to lead to cell death, we determined if drugs within each class were enriched in either the ineffective or effective categories by calculating the Pearson residual for each class (Supplementary Fig. S2B). Most drug classes were enriched with either effective or ineffective drugs, providing evidence that drugs with the same targets had similar effects. Anthracyclines, vinca alkaloids, and all drugs targeting Aurora kinases, histone deacetylase (HDAC), microtubules, pyruvate dehydrogenase kinase 1 (PDK1), fibroblast growth factor receptors (FGFR), CDC7, Bruton Tyrosine Kinase (BTK1), or the proteasome were effective, whereas those targeting matrix metalloproteinase, nitrogen oxide synthetase, or poly (ADP-ribose) polymerase (PARP) were ineffective. To determine whether effective drugs within the same target class cluster together, we performed unsupervised drug clustering of the effective drugs using their AOC_LD values (Supplementary Fig. S2C, D).

About half of the chemotherapy agents we tested were effective (43/78; 55%). To further classify the effectiveness of these chemotherapy agents, we divided them into 7 categories based on their mechanisms. The taxanes, anthracyclines, topoisomerase inhibitors, and vinca alkaloids were almost universally effective, whereas most of the alkylating agents and platinum drugs were largely ineffective (Supplementary Fig. 2B). Unsupervised clustering of the effective chemotherapy drugs according to their AOC_LD values demonstrated that drugs in the same category were more likely to cluster together than to cluster with drugs in a different class (Supplementary Fig. S3A, B). Likewise, we divided the drugs targeting the PI3K/AKT/mTOR pathway into 7 categories based on their targets. Most mTOR and PDK1 inhibitors were effective, and the drugs in the other categories had variable efficacy (Supplementary Fig. 2B). Drugs did not strongly cluster by target within the PI3K/AKT/mTOR group (Supplementary Fig. S3C, D) likely because of off-target effects and target overlap.

### Aurora kinase inhibitors are effective against HPV-positive cancers

To determine if any drug or drug class was more effective than the others against HPV-driven cancers, we first compared the number of HPV-positive and -negative cell lines that were sensitive to the 439 effective drugs to the number of HPV-positive and -negative cell lines that were resistant. Only 30 (7%) of the effective drugs had a differential effect based on HPV status, and only one class of drugs, the Aurora kinase inhibitors, was significantly more effective in HPV-positive cell lines ($P<0.05$, Fisher exact test; Fig. 1A, B).

Drugs from 15 classes were more effective in HPV-positive cell lines than in HPV-negative cell lines (Table S4). We closely examined all the effective drugs in each of these 15 classes to determine if there was a trend for a class effect that warranted further investigation (Supplementary Fig. S4A). Drugs from 2 of these classes (antimetabolites and MAPK inhibitors) had variable effects, with some drugs more effective in HPV-negative cell lines and others more effective in HPV-positive cell lines. Most drug classes (antimetabolites and inhibitors of CDK, PKC, PDGFR/KIT, MAPK, proteasome, JAK/STAT, PI3K/AKT/MTOR, topoisomerase, or VEGFR) did not demonstrate a class effect, as a minority of the drugs in these classes demonstrated a differential effect based on HPV status, and the direction of the effect was variable within the class. We did not study several drug classes (BTK, ATM, and metabolism inhibitors) further because of their overall lack of class efficacy. Within the large family of PI3K/AKT/MTOR inhibitors, several mTOR inhibitors were more effective in HPV-positive cell lines than in HPV-negative ones, but the overall efficacy of these drugs was low with the exception of Torin-2, which has several off-target effects at a concentration of 3.16μM. The more specific mTOR inhibitors—everolimus, rapamycin, and ridaforolimus—caused cell death only in a single cell line at concentrations known to inhibit mTOR (11,25). Likewise, drugs affecting microtubules were consistently more effective in HPV-positive cell lines, but in contrast to the mTOR inhibitors, every drug in the microtubule/taxane class caused cell death in most of the cell lines tested, including the HPV-negative cell lines. Only one microtubule/taxane was significantly more effective in HPV-positive than in HPV-negative cell lines. Consistent with our findings, taxanes have been shown to have broad clinical efficacy in squamous cancers (26,27).

All 16 Aurora kinase inhibitors tended to be more effective in HPV-positive cell lines, although the difference was statistically significant for only 7 of them when we used AOC_LD as a dichotomous variable (Fig. 1C). Three other drugs in the HTDS also inhibited Aurora kinases: the JAK3 inhibitor AT9283, the CDK2 inhibitor JNJ7706621, and hesperidin, which inhibits multiple targets. All 3 drugs were more effective in HPV-positive than in HPV-negative cell lines (Supplementary Fig. S4B). Likewise, when AOC_LD was used as a continuous variable, the difference was statistically significant ($P \leq 0.05$, Wilcoxon test) for 7 of the Aurora kinase inhibitors and for hesperidin, AT9283, and JNJ7706621 (Supplementary Fig. S4C). In addition to the AOC_LD values, we computed the $IC_{50}$ values of all 16 Aurora kinase inhibitors in HPV-positive cell lines (Supplementary Fig. S4D–E). Similar to our AOC_LD metric, most $IC_{50}$ values for Aurora kinase inhibitors are low in HPV-positive cell lines.

## Aurora kinase inhibitors cause apoptosis in HPV-positive cancer cells

To confirm that Aurora kinase inhibition led to cell death in HPV-positive cell lines, we examined the effect of 2 clinically relevant and specific drugs, alisertib (28) and barasertib (29), on apoptosis using 3 orthogonal methods and relevant drug concentrations. In addition to using a standard treatment time of 72 hours, we also treated the cells for 2 doubling times to overcome the artifact of a fixed treatment time for cell cycle–specific drugs in cell lines with diverse cycling times (24,30). Terminal deoxynucleotidyl transferase dUTP nick end labeling (TUNEL)-positive apoptotic nuclei significantly increased in HPV-positive cancer cell lines (UMSCC47, CaSki, and MS751) treated for 72 hours or 2 doubling times. However, no appreciable levels of apoptosis were noted in matched HPV-negative cancer cell lines (UMSCC19, FaDu, and HN31; Fig. 2A). Likewise, apoptosis induced by barasertib or alisertib was associated with selective caspase-3 activation and PARP cleavage in HPV-positive cancer cell lines (Figs. 2B, C). In contrast, no significant differences in senescence induced by Aurora kinase inhibitors were noted between HPV-positive cells and HPV-negative cells (Fig. 2D).

To test the effect of Aurora kinase inhibition *in vivo*, three patient-derived xenograft (PDX) models that were derived from patients with p16-positive oropharynx cancer [HOSC144 (HPV16, HPV52), HOSC19 (HPV18, HPV59), and HOSC 156 (HPV18)], were implanted in nude mice. We administered a low dose of alisertib (10 mg/kg) continuously for 3 weeks. In agreement with the *in vitro* findings, clear evidence of tumor regression was observed in both PDX models. This anti-tumor effect was accompanied by a concordant increase in survival duration (Figs. 3A–C). In addition, we also tested an HPV-negative cell line with high Rb protein levels and observed that it was resistant to alisertib treatment (Fig 3D). Also, a sustained response was observed even after treatment was stopped. Tumors collected from alisertib-treated mice on days 8 and 21 had significantly lower levels of Ki67 staining and increased levels of cleaved caspase-3 compared to those from vehicle-treated mice (Figs. 3E, F).

## Rb expression and *TP53* mutations predict cells' response to Aurora kinase inhibitors

To determine if factors other than HPV status predict response to Aurora kinase inhibitors, we compared protein expression using Reverse Phase Protein Arrays (RPPA) and gene mutation using whole exome sequencing (WES) to drug efficacy using AOC_LD. The expression levels of 19 proteins were correlated with sensitivity to at least 4 Aurora kinase inhibitors (Supplementary Fig. S5A) after correction for multiple testing ($P \leq 0.05$, adjusted for the false discovery rate). We used immunoblotting to validate the RPPA findings in all 33 cells lines. Among the 19 proteins, we focused on the 8 that correlated with sensitivity to the most drugs and in which the correlations were consistently in a single direction (i.e., expression predicted sensitivity or resistance but not both). On the basis of published studies (30,31), we also used immunoblotting to explore 7 additional candidate proteins that were not in our RPPA. Of the 15 chosen proteins, we were able to detect distinct immunoblotting bands for all except Tau. Only Rb, pRb (S807/811), and p16 were consistently correlated with drug sensitivity ($P \leq 0.05$ per the Wilcoxon test; Figs. 4A, Supplementary Figs S5B, C and S6; some data not shown). Specifically, the expression of pRb (S807/811) determined using RPPAs or immunoblotting, total Rb determined using immunoblotting,

and p16 (CDKN2A) determined using immunoblotting were correlated with the efficacy of all the Aurora kinase inhibitors, with statistical significance in 6, 6, 10, and 7 of the drugs, respectively (Supplementary Fig. S5C and Fig. S6; some data not shown). In addition, we also compared the pRb levels with sensitivity (AOC_LD) to 15 Aurora kinase inhibitors in only the HPV-positive cell lines. Although pRb (S807/811) expression is consistently lower in sensitive cell lines, the result did not reach statistical significance likely due to the low sample size (Supplementary Fig S6C).

We determined the extent to which drug sensitivity was correlated with 50 of the most common gene mutations in HNSCC (7). Only 35 of the 50 gene mutations were found in 2 or more cell lines in the HTDS. Of those 35 gene mutations, only *TP53* mutations were correlated with resistance to 7 Aurora kinase inhibitors (Supplementary Fig. S7A). Aurora B mRNA, Aurora B protein, and Aurora A mRNA expression did not correlate with Aurora kinase inhibitor efficacy (representative data, Supplementary Fig. S7B).

## Manipulation of RB1 affects Aurora kinase inhibition–induced apoptosis in squamous cancers

To determine if Rb protein expression is instrumental in Aurora kinase inhibitor–induced apoptosis, we used three independent methods to alter Rb expression in HPV-negative squamous cancer cell lines. First, we treated HPV-negative cells with alisertib and depleted the RB1 levels using transient transfection (Supplementary Fig. S8A). Rb depleted HPV-negative cells showed an increase in cleaved PARP levels upon treatment with alisertib. Next, we moved to a more stable system and knocked down *RB1* using short hairpin RNA (shRNA) that significantly reduced Rb protein expression in 3 HPV-negative cell lines (Supplementary Figs. S8B, C). Alisertib led to an approximately 3-fold increase in annexin V–positive apoptotic cells when Rb was depleted (Fig. 4B). Additionally, alisertib alone did not induce apoptosis in control cells with detectable Rb protein levels. However, alisertib induced significant apoptosis in those same cell lines with reduced Rb levels, as evidenced by cleaved caspase-3 and cleaved PARP (Fig. 4C). To reduce Rb protein levels using an independent method that recapitulated the HPV phenotype, we used a stable plasmid to induce E7 expression. This method caused Rb protein degradation in 2 HPV-negative cell lines (Supplementary Fig. S8D). As expected, the *RB1* RNA levels remained unchanged (Supplementary Fig. S8E). Alisertib treatment selectively enhanced apoptosis in cells overexpressing E7, as indicated by cleaved caspase-3 and PARP levels (Fig. 4D and Supplementary Fig. S8F) and annexin V (Fig. 4E and Supplementary Fig. S8G).

We also checked the effect of *RB1* silencing on the expression of other RB family members (RBL1, RBL2). We observed that the levels of RBL1 remained unchanged with the treatment. However, the protein levels of RBL2 decreased with RB1 silencing as well as with alisertib treatment (Supplementary Fig S8A). The effect of *RB1* silencing on RBL2 was likely due to pooled siRNAs. Using *RB1* shRNA, we did not observe an effect of RB1 depletion on RBL2, but we still observed the enhanced alisertib-induced apoptosis supporting a role for RB1 alone in this effect (Supplementary Fig S8H).

We noted a decrease of Rb protein expression following Aurora kinase inhibition that may be related to G2/M cell cycle arrest. Alternatively, it may be that the HPV negative

cells with low Rb expression are the ones that survive after Aurora inhibition. To test this at the single cell level, two HPV-negative cell lines were co-stained with anti-Rb labelled with FITC conjugate and anti-cleaved caspase-3 labelled with TRITC and treated with alisertib or vehicle control. As expected in these unsynchronized cells, Rb expression was detectable, but modestly heterogeneous in control cells. Consistent with the Western blots, Rb expression was notably lower and cleaved caspase 3 slightly higher in the alisertib-treated cells than in control cells. Consistent with our prior data, cells with higher Rb levels have no or very low levels of cleaved caspase-3. Cells with lower Rb levels have modest levels of cleaved caspase-3 (Supplementary Fig S8I).

We hypothesized that increased Rb expression can rescue HPV-positive cells from Aurora kinase inhibition–induced apoptosis. Inducing Rb expression using a stable or inducible plasmid was not successful because the existing E7 led to Rb protein degradation. To overcome this problem, we knocked down E7 expression using small interfering RNA (siRNA), which resulted in a 3-fold increase in Rb protein levels. As expected, alisertib treatment caused apoptosis in the HPV-positive cell lines but not in the same cells with increased Rb expression (Fig. 4F).

## Aurora kinase inhibition–induced apoptosis depends upon a balance of mitotic checkpoint proteins in Rb-deficient squamous cancers

In addition to having a well-characterized role in controlling entry into S phase, the inhibition of the Rb tumor suppressor pathway and subsequent activation of E2F directly enhance the expression of the mitotic checkpoint gene Mad2 and prolong mitosis (30,32–36). *MAD2L1* (Mad2) has a core E2F transcription factor binding site in its promoter and Rb-deficient cancer cells have elevated levels of Mad2 (34). The primed mitotic checkpoint complex (MCC) may create an Achilles heel for cancer cells lacking Rb because these cells depend on Aurora kinase activity to promote mitotic exit and survival. To test the hypothesis that Mad2 and BUB1B mediate Aurora kinase inhibitor sensitivity, we used siRNA to deplete their levels in 2 HPV-positive cell lines. In both cell lines, reduced levels of Mad2 or BUB1B rescued the cells from alisertib-induced apoptosis (Fig. 5A).

In normal cells, prolonged mitosis resulting from Mad2 overexpression can lead to G1 arrest or mitotic cell death (37,38), so it is unclear why Mad2 overexpression is tolerated in HPV-positive cancers. One potential mechanism to prevent stalled mitosis is the regulation of Mad2 function via TRIP13. We hypothesized that HPV-positive cells have an increased dependency on TRIP13 for their mitotic exit. Therefore, we induced the transient overexpression of TRIP13 in 2 HPV-positive cell lines and observed a partial rescue from alisertib-induced apoptosis as indicated by PARP and caspase-3 cleavage (Fig. 5B) and annexin V expression (Fig. 5C). Similarly, TRIP13 overexpression in 2 HPV-negative cell lines with RB1 knockdown (done with shRNA) reduced apoptosis caused by Aurora kinase inhibition (Fig. 5D).

MCC gene expression has never been examined in HPV-positive tumors. To determine if MCC genes are overexpressed in HPV-driven tumors, we examined their expression in tumor samples from 517 HNSCC patients in The Cancer Genome Atlas (TCGA) (7). We compared mRNA expression between 70 HPV-positive and 447 HPV-negative tumors and

found significantly higher expression of both *BUB1B* (BUBR1, BUB1β) and *MAD2L1* (Mad2) in HPV-positive tumors ($P$ <0.0001; Fig. 6A). We also compared only HPV-positive (n=51) and HPV-negative oropharynx squamous cell carcinoma (OPSCC, n=28) and found significantly higher expression of both *BUB1B* and *MAD2L1* in HPV-positive OPSCC tumors, P<0.05. (Fig 6A, right panel). The expression of *TRIP13* was lower in HPV positive than in HPV negative OPSCC, but the difference was not significant in both the sample sets. Specific case IDs for groups of TCGA patients with HNSCC and OPSCC are provided in Table S5 and Table S6.

Next we determined if *TRIP13, MAD2L1*, and *BUB1B* expression predicted response to Aurora kinase inhibition in HPV-positive cancer cells. We compared the mRNA expression of *TRIP13, MAD2L1*, and *BUB1B* to Aurora kinase inhibitor sensitivity. Consistent with our model, higher levels of *TRIP13* and lower levels of *BUB1B* predicted resistance, although the correlation did not reach statistical significance for most of the drugs likely due to a low sample size (Supplementary Figs. S9A–C).

## TRIP13 knockdown enhances Aurora kinase inhibition–induced cell death in HPV-positive squamous cancers

TRIP13 is an enzyme that is potentially a therapeutic target. To determine if Aurora kinase and TRIP13 inhibition have synthetic lethality in HPV-positive cancers, first we transfected HPV-positive cells with two different siRNAs against TRIP13 that reduced the expression of the TRIP13 mRNA and protein levels (Supplementary Figs S9D–G). Densitometric analysis of the band intensities showed that both siRNAs decreased TRIP13 expression by more than 50% (**, P<0.001) compared to control si-RNA (Supplementary Fig S9E). Next, we transfected both HPV-positive and HPV-negative cell lines with TRIP13 or control siRNA and treated them with low concentrations of alisertib. TRIP13 knockdown alone did not cause apoptosis, consistent with its effect in other cancer and normal cells (34). We observed higher levels of cleaved caspase-3 and cleaved PARP levels in HPV-positive cells transfected with TRIP13-knockdown with alisertib than in control cells treated with alisertib (Supplementary Fig S9G), whereas no expression of caspase-3 activation and PARP cleavage were observed in HPV-negative cells (Fig. 6B). In addition, the combination of TRIP13 knockdown with alisertib killed more than half of the cells from five HPV-positive cell lines without significantly affecting HPV-negative squamous cancer cells with wild type Rb (Fig. 6C) demonstrating selectivity. In addition, we also observed that the combination led to significant apoptosis in HPV positive cell lines that were resistant to alisertib (i.e., AOC-LD=0 in the HTDS) supporting our model (Fig. 6C). To determine if our model was applicable to other cancers with Rb pathway defects, we tested the combination of TRIP13 depletion and Aurora kinase inhibition in non-small cell lung cancer (NSCLC) cell lines with various levels of Rb expression. We found that cancer cells with low Rb levels experienced significantly more apoptosis with the combination than those with high Rb expression (Supplementary Figs S9H–J).

Next, we induced Mad2 overexpression in 2 HPV-positive cell lines to test if altering the balance between TRIP13 and Mad2 would affect cells' sensitivity to Aurora kinase

inhibition. Mad2 overexpression alone did not activate the apoptotic pathways. However, Mad2 overexpression combined with alisertib enhanced apoptosis (Figs. 6D, E).

This study provides strong evidence to support a model in which HPV positive cancer cells maintain a balance of Mad2 and TRIP13 allowing mitotic exit and survival despite Rb loss. The combined inhibition of TRIP13 and Aurora kinase disrupts the balance and leads to enhanced cell death in Rb-deficient HPV-positive cancer cells (Fig. 6F).

## DISCUSSION

In the current study, we sought to identify, validate, and characterize HPV status–selective therapy. We tested the ability of 864 diverse compounds to cause cell death in a large panel of HPV-positive and -negative squamous cancer cells. We identified Aurora kinase inhibitors as the drug class that was consistently more effective against HPV-positive cancers than HPV-negative cancers. Aurora kinase inhibition reduced tumor volume *in vivo* without toxicity. In addition to HPV status, baseline protein levels of Rb predicted the response to Aurora kinase inhibitors. Manipulating Rb expression altered sensitivity to Aurora kinase inhibitors. Further, our data identify a novel mechanism in which HPV-positive cancer cells maintain a balance of Mad2 and TRIP13 levels, allowing mitotic exit and survival despite Rb loss and Aurora kinase inhibition. Altering that balance enhanced Aurora kinase inhibition–induced apoptosis. Consistent with this observation, we found that a combination of TRIP13 knockdown with Aurora kinase inhibition led to marked apoptosis in HPV-positive cells, but not in HPV-negative cells that express Rb.

Our *in vivo* data from three, independent PDX models of HPV-driven HNSCC demonstrated not only a striking tumor regression and survival duration benefit with Aurora kinase inhibition but also a sustained response even after treatment was stopped. McMillan *et al.* were the first to demonstrate that targeting Aurora A enhanced sensitivity to alisertib in HPV-transformed cells (39–42). However, they did not uncover the mechanisms driving the selective sensitivity of HPV-positive cancers.

In the present study, we determined that low Rb levels drive sensitivity to Aurora kinase inhibitors. Our findings are consistent with those showing that other cancer types with *RB1* loss-of-function mutations depend on mitotic kinases—particularly Aurora B (31) and Aurora A (30)—for survival. The inhibition of Rb pathways upregulates MCC genes and can result in chromosomal instability and prolonged mitosis (35,43). We found that in HNSCC patients, *BUB1B* and *MAD2L1* expression was higher in HPV-positive than in HPV-negative tumors. Gong *et al.* demonstrated that *BUB1B* depletion partially rescues Rb-deficient small cell lung cancer (SCLC) cells from Aurora kinase A inhibition–induced apoptosis (30). Similarly, we found that the knockdown of Mad2 and BUB1B markedly reduced alisertib-induced apoptosis in HPV-positive squamous cancer cells.

To further investigate the mechanism of sensitivity to Aurora kinase inhibition and identify a potentially druggable target, we investigated the role of TRIP13 in HPV-positive cells. TRIP13 belongs to the AAA-ATPase family of chaperone proteins, which regulates the SAC by remodeling its effector, Mad2, from a “closed” (active) to an “open” (inactive)

form during mitosis (44). TRIP13 localizes to kinetochores, and its knockdown affects the ATPase activity that delays metaphase-to-anaphase transition. Cancer cells overexpressing Mad2 have an increased dependency on TRIP13 for their mitotic exit (34). Given that Mad2 is overexpressed in HPV-positive patient tumors, we hypothesized that the balance of Mad2 and TRIP13 dictates HPV-positive cancer cells' dependence on Aurora kinases for their mitotic exit and survival. In the present study, TRIP13 knockdown alone did not cause any significant cell death. However, the combined inhibition of TRIP13 and Aurora kinase had a synergistic effect and caused marked apoptosis. Interestingly, Mad2 overexpression enhanced alisertib-induced apoptosis to a lesser degree than did TRIP13 depletion, leading us to speculate that endogenous TRIP13 levels inactivate Mad2 to protect cells. This finding emphasized that Mad2 overexpression increases cells' dependency on TRIP13 for survival. In Rb-proficient cancers, disrupting mitosis may also affect the efficacy of Aurora kinase inhibition. Aurora kinase inhibitors alone do not cause cell death in HPV-negative HNSCC, but when combined with Wee1 inhibitors led to mitotic catastrophe (45).

While further works needs to be done to truly understand how the balance of TRIP13 and Mad2 levels mediates sensitivity to Aurora kinase inhibitors, we can take advantage of this relationship as a potential way to effectively target HPV-positive squamous cancer cells while sparing normal cells that express Rb and have unaltered levels of Mad2. The reduction of TRIP13 in normal cells causes only a mild mitotic delay without cell death. Even genetically engineered mice with loss of TRIP13 are viable and grossly normal, although they are smaller than their wild-type counterparts at birth (46). However, we found that, in HPV-positive cancer cells with high endogenous levels of Mad2, combined TRIP13 and Aurora kinase inhibition led to striking levels of apoptosis. This result suggests that TRIP13 could be therapeutically targeted, with potentially low toxicity, in tumors with high Mad2 levels. Given that TRIP13 is an AAA-ATPase, it is a more readily druggable target than Mad2 is. Other AAA-ATPases, such p97 and ATAD2, are clinically important targets in cancer and have been targeted with small molecules that have shown potential promise in many therapeutic regimens (47).

TRIP13 also functions in DNA repair by promoting nonhomologous end joining (NHEJ) and inducing treatment resistance by binding to the NHEJ proteins KU70, KU80, and DNA-PKcs in head and neck cancer (48). Studies have also suggested that the inhibition of Aurora kinases stimulates the error-prone NHEJ repair of DNA double-strand breaks with increased DNA-PKcs phosphorylation (49). Thus, to examine the synergistic effects of TRIP13 and Aurora kinase inhibition, we knocked down TRIP13 expression in cells and treated them with alisertib. TRIP13 inhibition enhanced the cytotoxic effects of alisertib in HPV-positive cells, which suggests that TRIP13 inhibition, in combination with other therapeutics, can reduce cancer cell survival.

Several other biomarkers of sensitivity to Aurora kinase inhibitors have been identified. SCLC cells with *MYC* amplification or high gene expression frequently respond to Aurora B inhibitors (29), although an independent study demonstrated that neither *MYC* expression nor amplification is required for sensitivity to Aurora A kinase inhibition in *RB1*-mutant SCLC cells (30). One potential mechanism of sensitivity to Aurora kinase inhibition is Myc's activation of Mad2 and BUBR1 (50). However, in our squamous cancer cell lines,

Myc protein expression did not correlate with sensitivity to Aurora kinase inhibitors, which suggests that Rb1 loss is the more important driver of Mad2 expression. Other potential biomarkers of Aurora kinase inhibitor sensitivity in HNSCC are mutations in *KMT2D* (lysine methyltransferase 2D) (12), although *KMT2D* mutations did not correlate with sensitivity in the current study, in which cell death, rather than inhibition of proliferation, was used as a metric of drug sensitivity. Previous studies have shown that methyltransferase regulates the SAC complex by directly binding to Mad2 and thereby limiting its availability (51). In HNSCC, mutations in *KMT2D* may create an imbalance of Mad2 and TRIP13 levels, which would make *KMT2D*-mutant cells dependent on Aurora kinases for their mitotic exit and survival.

One strength of our study is the use of cell death rather than a reduction in cell proliferation as a measure of drug efficacy. Our metric is not affected by the number of cell divisions during the assay. This difference may explain why we and others have identified distinct targets, such as Wee1, PLK1, and HDAC inhibitors, that are more effective in HPV-positive HNSCC using conventional $IC_{50}$ values (12,52). One limitation is that we used the same drug concentration range (0.01–3.16 μM) for all the drugs. This range may not have been appropriate for all the drugs in the screen.

To promote rapid translation of our research, we used alisertib for most of our studies because it is a specific inhibitor of Aurora A that is well-tolerated and under active clinical development. Alisertib has an established safety profile in human clinical trials (53–56). Common toxicities include anemia, thrombocytopenia, and neutropenia. Multiple clinical trials using Aurora kinase inhibition have not shown clinical efficacy of single agents in solid tumors. Indeed, even some HPV positive models experienced only minimal apoptosis with modest, clinically relevant concentrations of alisertib. However, our data demonstrate that the combination the TRIP13 and Aurora kinase inhibition will be effective in HPV positive cancers. The greatest unmet clinical need is for more effective systemic therapy for patients with recurrent/metastatic HNSCC that is resistant to cisplatin and/or radiotherapy. Several of the cell lines we used are resistant to cisplatin and radiotherapy. In HNSCC patients who received 100mg/$m^2$ cisplatin, the plasma $C_{max}$ was 11 μM (57). Several HPV+ cell lines have $IC_{50}$ values above 11 μM including SiHa (28 μM), ME180 (12 μM), CaSki (15 μM), (58), Vu147T (11.2 μM), UPCI-SCC-090 (11.1 μM) and UDSCC2 (18 μM) (59). Additionally, SiHa and UPCI-SCC090 are resistant to radiotherapy (58,60).

The data presented herein show that Aurora kinase and TRIP13 have synthetic lethality specifically in HPV-driven squamous cancer cells because the cells' loss of Rb protein expression leads to high Mad2 expression. HPV-positive tumors from patients with HNSCC also exhibited high levels of Mad2 expression. This cancer cell–specific effect allowed us to reduce the concentration of alisertib needed for treatment. This result suggests that the combination of TRIP13 and Aurora kinase inhibition provides a wider therapeutic window than classic cytotoxic agents do for the treatment of HPV-positive squamous cell carcinoma. This combination could help meet an urgent unmet need to reduce mortality and long-term treatment-related toxicity among patients with HPV-driven cancers. The findings may also be applicable to the treatment of patients with other cancers with Rb pathway defects, including NSCLC (61).

## Supplementary Material

Refer to Web version on PubMed Central for supplementary material.

## Acknowledgments:

We would like to thank all members of Flow cytometry & Cellular Imaging facility, which is supported in part by the National Institutes of Health through M.D. Anderson's Cancer Center Support Grant CA016672. We would also like to thank Laura L. Russell, scientific editor of MD Anderson, Research Medical Library, for editing this article.

**Funding:**

This work was supported by the National Institutes of Health (NIH) (R01CA248205; FMJ); philanthropic contributions from Mr. and Mrs. Charles W. Stiefel to The University of Texas MD Anderson Cancer Center-Oropharynx Cancer Program (FMJ, CRP); and the Cancer Prevention and Research Institute of Texas (RP150578; CS). This work used the services of MD Anderson's Flow Cytometry and Cellular Imaging Facility and Bioinformatics Shared Resource, which are supported by the NIH through MD Anderson's Cancer Center Support Grant (P30CA016672).

## References

1. de Martel C, Georges D, Bray F, Ferlay J, Clifford GM. Global burden of cancer attributable to infections in 2018: a worldwide incidence analysis. Lancet Glob Health 2020;8(2):e180–e90 doi 10.1016/S2214-109X(19)30488-7. [PubMed: 31862245]
2. Berman TA, Schiller JT. Human papillomavirus in cervical cancer and oropharyngeal cancer: One cause, two diseases. Cancer 2017;123(12):2219–29 doi 10.1002/cncr.30588. [PubMed: 28346680]
3. Chaturvedi AK, Anderson WF, Lortet-Tieulent J, Curado MP, Ferlay J, Franceschi S, et al. Worldwide trends in incidence rates for oral cavity and oropharyngeal cancers. J Clin Oncol 2013;31(36):4550–9 doi 10.1200/JCO.2013.50.3870. [PubMed: 24248688]
4. Gillison ML, Chaturvedi AK, Anderson WF, Fakhry C. Epidemiology of Human Papillomavirus-Positive Head and Neck Squamous Cell Carcinoma. J Clin Oncol 2015;33(29):3235–42 doi 10.1200/JCO.2015.61.6995. [PubMed: 26351338]
5. Mott FE, Sacks R, Johnson F, Hutcheson KA, Gallagher N, Varghese S, et al. Subjective functional outcomes in oropharyngeal cancer treated with induction chemotherapy using the MD Anderson Symptom Inventory (MDASI). Laryngoscope Investig Otolaryngol 2020;5(6):1104–9 doi 10.1002/lio2.487.
6. Mirghani H, Blanchard P. Treatment de-escalation for HPV-driven oropharyngeal cancer: Where do we stand? Clin Transl Radiat Oncol 2018;8:4–11 doi 10.1016/j.ctro.2017.10.005. [PubMed: 29594236]
7. Cancer Genome Atlas N Comprehensive genomic characterization of head and neck squamous cell carcinomas. Nature 2015;517(7536):576–82 doi 10.1038/nature14129. [PubMed: 25631445]
8. Gillison ML, Akagi K, Xiao W, Jiang B, Pickard RKL, Li J, et al. Human papillomavirus and the landscape of secondary genetic alterations in oral cancers. Genome Res 2019;29(1):1–17 doi 10.1101/gr.241141.118.
9. Bourgo RJ, Braden WA, Wells SI, Knudsen ES. Activation of the retinoblastoma tumor suppressor mediates cell cycle inhibition and cell death in specific cervical cancer cell lines. Mol Carcinog 2009;48(1):45–55 doi 10.1002/mc.20456. [PubMed: 18506774]
10. Zhao M, Sano D, Pickering CR, Jasser SA, Henderson YC, Clayman GL, et al. Assembly and initial characterization of a panel of 85 genomically validated cell lines from diverse head and neck tumor sites. Clin Cancer Res 2011;17(23):7248–64 doi 10.1158/1078-0432.CCR-11-0690. [PubMed: 21868764]
11. Mazumdar T, Byers LA, Ng PK, Mills GB, Peng S, Diao L, et al. A comprehensive evaluation of biomarkers predictive of response to PI3K inhibitors and of resistance mechanisms in head and neck squamous cell carcinoma. Mol Cancer Ther 2014;13(11):2738–50 doi 10.1158/1535-7163.MCT-13-1090. [PubMed: 25193510]

12. Kalu NN, Mazumdar T, Peng S, Tong P, Shen L, Wang J, et al. Comprehensive pharmacogenomic profiling of human papillomavirus-positive and -negative squamous cell carcinoma identifies sensitivity to aurora kinase inhibition in KMT2D mutants. Cancer Lett 2018;431:64–72 doi 10.1016/j.canlet.2018.05.029. [PubMed: 29807113]
13. Kalu NN, Mazumdar T, Peng S, Shen L, Sambandam V, Rao X, et al. Genomic characterization of human papillomavirus-positive and -negative human squamous cell cancer cell lines. Oncotarget 2017;8(49):86369–83 doi 10.18632/oncotarget.21174. [PubMed: 29156801]
14. Zhang M, Singh R, Peng S, Mazumdar T, Sambandam V, Shen L, et al. Mutations of the LIM protein AJUBA mediate sensitivity of head and neck squamous cell carcinoma to treatment with cell-cycle inhibitors. Cancer Lett 2017;392:71–82 doi 10.1016/j.canlet.2017.01.024. [PubMed: 28126323]
15. Ferrarotto R, Goonatilake R, Yoo SY, Tong P, Giri U, Peng S, et al. Epithelial-Mesenchymal Transition Predicts Polo-Like Kinase 1 Inhibitor-Mediated Apoptosis in Non-Small Cell Lung Cancer. Clin Cancer Res 2016;22(7):1674–86 doi 10.1158/1078-0432.CCR-14-2890. [PubMed: 26597303]
16. Schneider CA, Rasband WS, Eliceiri KW. NIH Image to ImageJ: 25 years of image analysis. Nature methods 2012;9(7):671–5 doi 10.1038/nmeth.2089. [PubMed: 22930834]
17. Peng S, Creighton CJ, Zhang Y, Sen B, Mazumdar T, Myers JN, et al. Tumor grafts derived from patients with head and neck squamous carcinoma authentically maintain the molecular and histologic characteristics of human cancers. J Transl Med 2013;11:198 doi 10.1186/1479-5876-11-198. [PubMed: 23981300]
18. Chaturvedi AK, Graubard BI, Pickard RKL, Xiao W, Gillison ML. High-Risk Oral Human Papillomavirus Load in the US Population, National Health and Nutrition Examination Survey 2009–2010. The Journal of Infectious Diseases 2014;210(3):441–7 doi 10.1093/infdis/jiu116. [PubMed: 24625808]
19. Fakhry C, Blackford AL, Neuner G, Xiao W, Jiang B, Agrawal A, et al. Association of Oral Human Papillomavirus DNA Persistence With Cancer Progression After Primary Treatment for Oral Cavity and Oropharyngeal Squamous Cell Carcinoma. JAMA Oncol 2019;5(7):985–92 doi 10.1001/jamaoncol.2019.0439. [PubMed: 31046104]
20. Kaplan EL, Meier P. Nonparametric-Estimation from Incomplete Observations. Journal of the American Statistical Association 1958;53(282):457–81 doi Doi 10.2307/2281868.
21. Vivian J, Rao AA, Nothaft FA, Ketchum C, Armstrong J, Novak A, et al. Toil enables reproducible, open source, big biomedical data analyses. Nat Biotechnol 2017;35(4):314–6 doi 10.1038/nbt.3772. [PubMed: 28398314]
22. Chen Y, Yao H, Thompson EJ, Tannir NM, Weinstein JN, Su X. VirusSeq: software to identify viruses and their integration sites using next-generation sequencing of human cancer tissue. Bioinformatics 2013;29(2):266–7 doi 10.1093/bioinformatics/bts665. [PubMed: 23162058]
23. Gleber-Netto FO, Rao X, Guo T, Xi Y, Gao M, Shen L, et al. Variations in HPV function are associated with survival in squamous cell carcinoma. JCI Insight 2019;4(1) doi 10.1172/jci.insight.124762.
24. Hafner M, Niepel M, Chung M, Sorger PK. Growth rate inhibition metrics correct for confounders in measuring sensitivity to cancer drugs. Nature methods 2016;13(6):521–7 doi 10.1038/nmeth.3853. [PubMed: 27135972]
25. Sambandam V, Frederick MJ, Shen L, Tong P, Rao X, Peng S, et al. PDK1 Mediates NOTCH1-Mutated Head and Neck Squamous Carcinoma Vulnerability to Therapeutic PI3K/mTOR Inhibition. Clin Cancer Res 2019;25(11):3329–40 doi 10.1158/1078-0432.CCR-18-3276. [PubMed: 30770351]
26. Misiukiewicz K, Gupta V, Bakst R, Posner M. Taxanes in cancer of the head and neck. Anticancer Drugs 2014;25(5):561–70 doi 10.1097/CAD.0000000000000086. [PubMed: 24534821]
27. Shin DM, Lippman SM. Paclitaxel-based chemotherapy for recurrent and/or metastatic head and neck squamous cell carcinoma: current and future directions. Semin Oncol 1999;26(1 Suppl 2):100–5. [PubMed: 10190789]
28. Manfredi MG, Ecsedy JA, Chakravarty A, Silverman L, Zhang M, Hoar KM, et al. Characterization of Alisertib (MLN8237), an investigational small-molecule inhibitor of aurora

A kinase using novel in vivo pharmacodynamic assays. Clin Cancer Res 2011;17(24):7614–24 doi 10.1158/1078-0432.CCR-11-1536. [PubMed: 22016509]

29. Helfrich BA, Kim J, Gao D, Chan DC, Zhang Z, Tan AC, et al. Barasertib (AZD1152), a Small Molecule Aurora B Inhibitor, Inhibits the Growth of SCLC Cell Lines In Vitro and In Vivo. Mol Cancer Ther 2016;15(10):2314–22 doi 10.1158/1535-7163.MCT-16-0298. [PubMed: 27496133]
30. Gong X, Du J, Parsons SH, Merzoug FF, Webster Y, Iversen PW, et al. Aurora A Kinase Inhibition Is Synthetic Lethal with Loss of the RB1 Tumor Suppressor Gene. Cancer Discov 2019;9(2):248–63 doi 10.1158/2159-8290.CD-18-0469. [PubMed: 30373917]
31. Oser MG, Fonseca R, Chakraborty AA, Brough R, Spektor A, Jennings RB, et al. Cells Lacking the RB1 Tumor Suppressor Gene Are Hyperdependent on Aurora B Kinase for Survival. Cancer Discov 2019;9(2):230–47 doi 10.1158/2159-8290.CD-18-0389. [PubMed: 30373918]
32. Manning AL, Dyson NJ. RB: mitotic implications of a tumour suppressor. Nat Rev Cancer 2012;12(3):220–6 doi 10.1038/nrc3216. [PubMed: 22318235]
33. Hernando E, Nahle Z, Juan G, Diaz-Rodriguez E, Alaminos M, Hemann M, et al. Rb inactivation promotes genomic instability by uncoupling cell cycle progression from mitotic control. Nature 2004;430(7001):797–802 doi 10.1038/nature02820. [PubMed: 15306814]
34. Marks DH, Thomas R, Chin Y, Shah R, Khoo C, Benezra R. Mad2 Overexpression Uncovers a Critical Role for TRIP13 in Mitotic Exit. Cell Rep 2017;19(9):1832–45 doi 10.1016/j.celrep.2017.05.021. [PubMed: 28564602]
35. Carter SL, Eklund AC, Kohane IS, Harris LN, Szallasi Z. A signature of chromosomal instability inferred from gene expression profiles predicts clinical outcome in multiple human cancers. Nat Genet 2006;38(9):1043–8 doi 10.1038/ng1861. [PubMed: 16921376]
36. Schvartzman JM, Sotillo R, Benezra R. Mitotic chromosomal instability and cancer: mouse modelling of the human disease. Nat Rev Cancer 2010;10(2):102–15 doi 10.1038/nrc2781. [PubMed: 20094045]
37. Vogel C, Kienitz A, Hofmann I, Muller R, Bastians H. Crosstalk of the mitotic spindle assembly checkpoint with p53 to prevent polyploidy. Oncogene 2004;23(41):6845–53 doi 10.1038/sj.onc.1207860. [PubMed: 15286707]
38. Gascoigne KE, Taylor SS. Cancer cells display profound intra- and interline variation following prolonged exposure to antimitotic drugs. Cancer Cell 2008;14(2):111–22 doi 10.1016/j.ccr.2008.07.002. [PubMed: 18656424]
39. Gabrielli B, Bokhari F, Ranall MV, Oo ZY, Stevenson AJ, Wang W, et al. Aurora A Is Critical for Survival in HPV-Transformed Cervical Cancer. Mol Cancer Ther 2015;14(12):2753–61 doi 10.1158/1535-7163.MCT-15-0506. [PubMed: 26516156]
40. Shaikh MH, Idris A, Johnson NW, Fallaha S, Clarke DTW, Martin D, et al. Aurora kinases are a novel therapeutic target for HPV-positive head and neck cancers. Oral Oncol 2018;86:105–12 doi 10.1016/j.oraloncology.2018.09.006. [PubMed: 30409290]
41. Martin D, Fallaha S, Proctor M, Stevenson A, Perrin L, McMillan N, et al. Inhibition of Aurora A and Aurora B Is Required for the Sensitivity of HPV-Driven Cervical Cancers to Aurora Kinase Inhibitors. Mol Cancer Ther 2017;16(9):1934–41 doi 10.1158/1535-7163.MCT-17-0159. [PubMed: 28522591]
42. Tayyar Y, Idris A, Vidimce J, Ferreira DA, McMillan NA. Alpelisib and radiotherapy treatment enhances Alisertib-mediated cervical cancer tumor killing. Am J Cancer Res 2021;11(6):3240–51. [PubMed: 34249458]
43. Schvartzman JM, Duijf PH, Sotillo R, Coker C, Benezra R. Mad2 is a critical mediator of the chromosome instability observed upon Rb and p53 pathway inhibition. Cancer Cell 2011;19(6):701–14 doi 10.1016/j.ccr.2011.04.017. [PubMed: 21665145]
44. Ye Q, Kim DH, Dereli I, Rosenberg SC, Hagemann G, Herzog F, et al. The AAA+ ATPase TRIP13 remodels HORMA domains through N-terminal engagement and unfolding. EMBO J 2017;36(16):2419–34 doi 10.15252/embj.201797291. [PubMed: 28659378]
45. Lee JW, Parameswaran J, Sandoval-Schaefer T, Eoh KJ, Yang DH, Zhu F, et al. Combined Aurora Kinase A (AURKA) and WEE1 Inhibition Demonstrates Synergistic Antitumor Effect in Squamous Cell Carcinoma of the Head and Neck. Clin Cancer Res 2019;25(11):3430–42 doi 10.1158/1078-0432.CCR-18-0440. [PubMed: 30755439]

46. Li XC, Schimenti JC. Mouse pachytene checkpoint 2 (trip13) is required for completing meiotic recombination but not synapsis. PLoS genetics 2007;3(8):e130 doi 10.1371/journal.pgen.0030130. [PubMed: 17696610]
47. Zhou HJ, Wang J, Yao B, Wong S, Djakovic S, Kumar B, et al. Discovery of a First-in-Class, Potent, Selective, and Orally Bioavailable Inhibitor of the p97 AAA ATPase (CB-5083). J Med Chem 2015;58(24):9480–97 doi 10.1021/acs.jmedchem.5b01346. [PubMed: 26565666]
48. Banerjee R, Russo N, Liu M, Basrur V, Bellile E, Palanisamy N, et al. TRIP13 promotes error-prone nonhomologous end joining and induces chemoresistance in head and neck cancer. Nature communications 2014;5:4527 doi 10.1038/ncomms5527.
49. Do TV, Hirst J, Hyter S, Roby KF, Godwin AK. Aurora A kinase regulates non-homologous end-joining and poly(ADP-ribose) polymerase function in ovarian carcinoma cells. Oncotarget 2017;8(31):50376–92 doi 10.18632/oncotarget.18970. [PubMed: 28881569]
50. Menssen A, Epanchintsev A, Lodygin D, Rezaei N, Jung P, Verdoodt B, et al. c-MYC delays prometaphase by direct transactivation of MAD2 and BubR1: identification of mechanisms underlying c-MYC-induced DNA damage and chromosomal instability. Cell Cycle 2007;6(3):339–52 doi 10.4161/cc.6.3.3808. [PubMed: 17297307]
51. Schibler A, Koutelou E, Tomida J, Wilson-Pham M, Wang L, Lu Y, et al. Histone H3K4 methylation regulates deactivation of the spindle assembly checkpoint through direct binding of Mad2. Genes Dev 2016;30(10):1187–97 doi 10.1101/gad.278887.116. [PubMed: 27198228]
52. Tanaka N, Patel AA, Wang J, Frederick MJ, Kalu NN, Zhao M, et al. Wee-1 Kinase Inhibition Sensitizes High-Risk HPV+ HNSCC to Apoptosis Accompanied by Downregulation of MCl-1 and XIAP Antiapoptotic Proteins. Clin Cancer Res 2015;21(21):4831–44 doi 10.1158/1078-0432.CCR-15-0279. [PubMed: 26124202]
53. Dickson MA, Mahoney MR, Tap WD, D'Angelo SP, Keohan ML, Van Tine BA, et al. Phase II study of MLN8237 (Alisertib) in advanced/metastatic sarcoma. Ann Oncol 2016;27(10):1855–60 doi 10.1093/annonc/mdw281. [PubMed: 27502708]
54. Venkatakrishnan K, Zhou X, Ecsedy J, Mould DR, Liu H, Danaee H, et al. Dose selection for the investigational anticancer agent alisertib (MLN8237): Pharmacokinetics, pharmacodynamics, and exposure-safety relationships. J Clin Pharmacol 2015;55(3):336–47 doi 10.1002/jcph.410. [PubMed: 25302940]
55. Venkatakrishnan K, Kim TM, Lin CC, Thye LS, Chng WJ, Ma B, et al. Phase 1 study of the investigational Aurora A kinase inhibitor alisertib (MLN8237) in East Asian cancer patients: pharmacokinetics and recommended phase 2 dose. Invest New Drugs 2015;33(4):942–53 doi 10.1007/s10637-015-0258-y. [PubMed: 26084989]
56. Melichar B, Adenis A, Lockhart AC, Bennouna J, Dees EC, Kayaleh O, et al. Safety and activity of alisertib, an investigational aurora kinase A inhibitor, in patients with breast cancer, small-cell lung cancer, non-small-cell lung cancer, head and neck squamous-cell carcinoma, and gastro-oesophageal adenocarcinoma: a five-arm phase 2 study. Lancet Oncol 2015;16(4):395–405 doi 10.1016/S1470-2045(15)70051-3. [PubMed: 25728526]
57. Chargi N, Molenaar-Kuijsten L, Huiskamp LFJ, Devriese LA, de Bree R, Huitema ADR. The association of cisplatin pharmacokinetics and skeletal muscle mass in patients with head and neck cancer: The prospective PLATISMA study. Eur J Cancer 2022;160:92–9 doi 10.1016/j.ejca.2021.10.010. [PubMed: 34810046]
58. Saxena A, Yashar C, Taylor DD, Gercel-Taylor C. Cellular response to chemotherapy and radiation in cervical cancer. American journal of obstetrics and gynecology 2005;192(5):1399–403 doi 10.1016/j.ajog.2004.12.045. [PubMed: 15902120]
59. Leonard BC, Lee ED, Bhola NE, Li H, Sogaard KK, Bakkenist CJ, et al. ATR inhibition sensitizes HPV(−) and HPV(+) head and neck squamous cell carcinoma to cisplatin. Oral Oncol 2019;95:35–42 doi 10.1016/j.oraloncology.2019.05.028. [PubMed: 31345392]
60. Nagel R, Martens-de Kemp SR, Buijze M, Jacobs G, Braakhuis BJ, Brakenhoff RH. Treatment response of HPV-positive and HPV-negative head and neck squamous cell carcinoma cell lines. Oral Oncol 2013;49(6):560–6 doi 10.1016/j.oraloncology.2013.03.446. [PubMed: 23578372]
61. Knudsen ES, Nambiar R, Rosario SR, Smiraglia DJ, Goodrich DW, Witkiewicz AK. Pan-cancer molecular analysis of the RB tumor suppressor pathway. Commun Biol 2020;3(1):158 doi 10.1038/s42003-020-0873-9. [PubMed: 32242058]

## Statement of translational relevance

HPV-driven cancers, which are Rb-deficient due to the expression of the viral protein E7, depend upon the mitotic checkpoint complex for survival following Aurora kinase inhibition. This vulnerability results in a selective sensitivity to the combination of Aurora kinase inhibition and depletion of the MAD2L1 regulator TRIP13. This combination, which to our knowledge has not been investigated for the treatment of any cancer, resulted in substantial cancer cell death in HPV-positive but not HPV-negative cancer cells and may thus improve rates of durable clinical responses. By sparing normal cells that express Rb and have unaltered levels of MAD2L1, this combination may reduce treatment toxicity among patients with HPV-positive cancer. The findings may also be applicable to the treatment of patients with other cancers with Rb pathway defects, including non-small cell lung cancer.

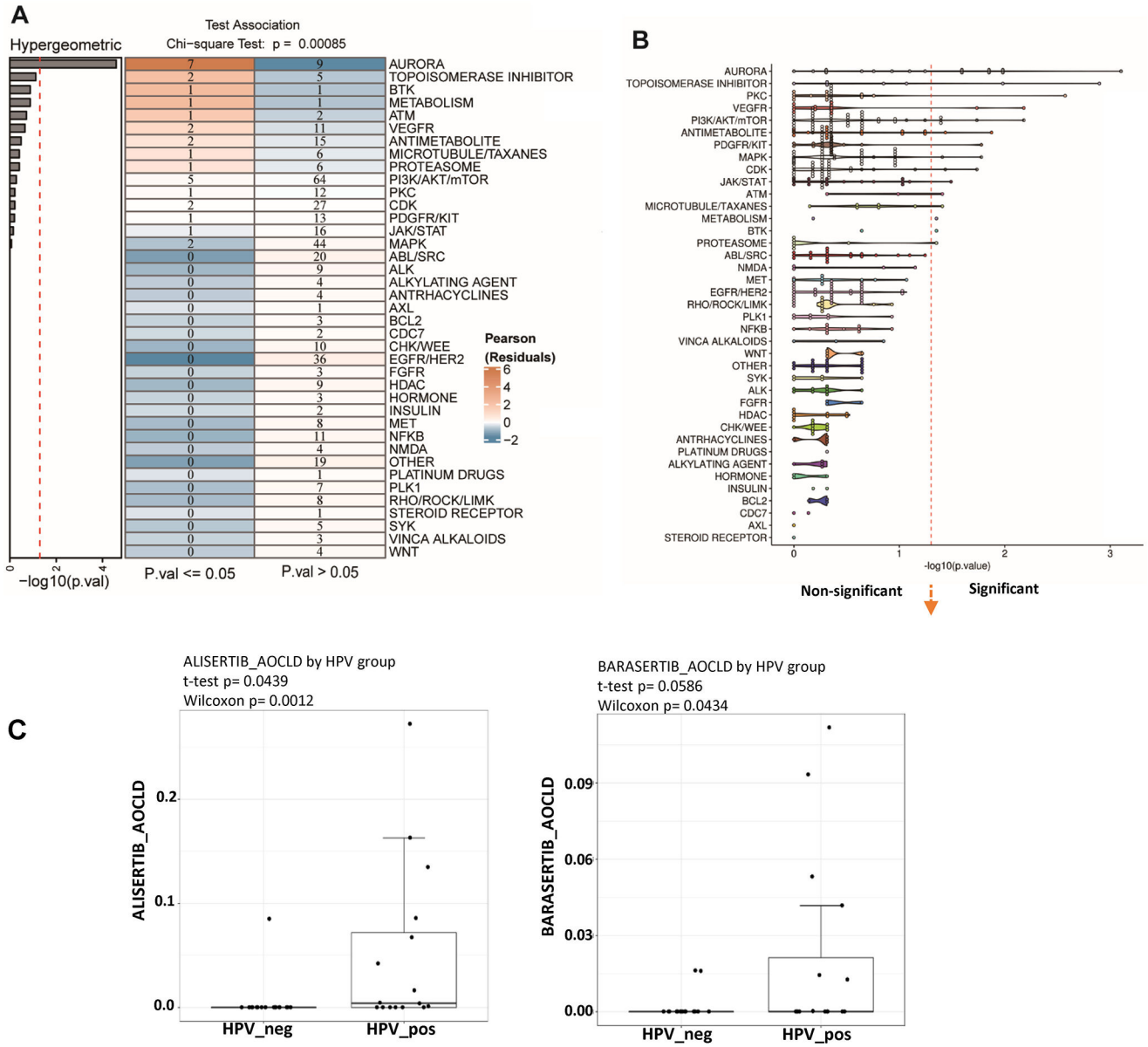


**Figure. 1. Aurora kinase inhibitors are effective in HPV-positive squamous carcinoma cell lines.**

**A,** The differential efficacies of 439 effective drugs based on HPV status were compared. Only 30 drugs (left column) demonstrated a significantly different effect ($P \leq 0.05$). The number in each cell corresponds to the number of drugs in each category, and the color of each cell corresponds to the standardized Pearson residual measuring the strength of enrichment for the drugs allocated to each category. Orange indicates enrichment. Blue indicates depletion. The histogram on the left shows the hypergeometric log10 $P$ values; the red dashed line indicates $P = 0.05$. **B,** The hypergeometric log10 $P$ values for 439 drugs are shown for the drugs divided into 39 categories. The dashed red line indicates $P = 0.05$. **C,** AOC_LD values for 2 Aurora kinase inhibitors, alisertib and barasertib. The AOC_LD values were used as continuous variables, and cell lines were grouped by HPV status. Box

plots show the median AOC_LD levels and 95% confidence intervals across all cell lines in each category. Each data point represents 1 cell line.

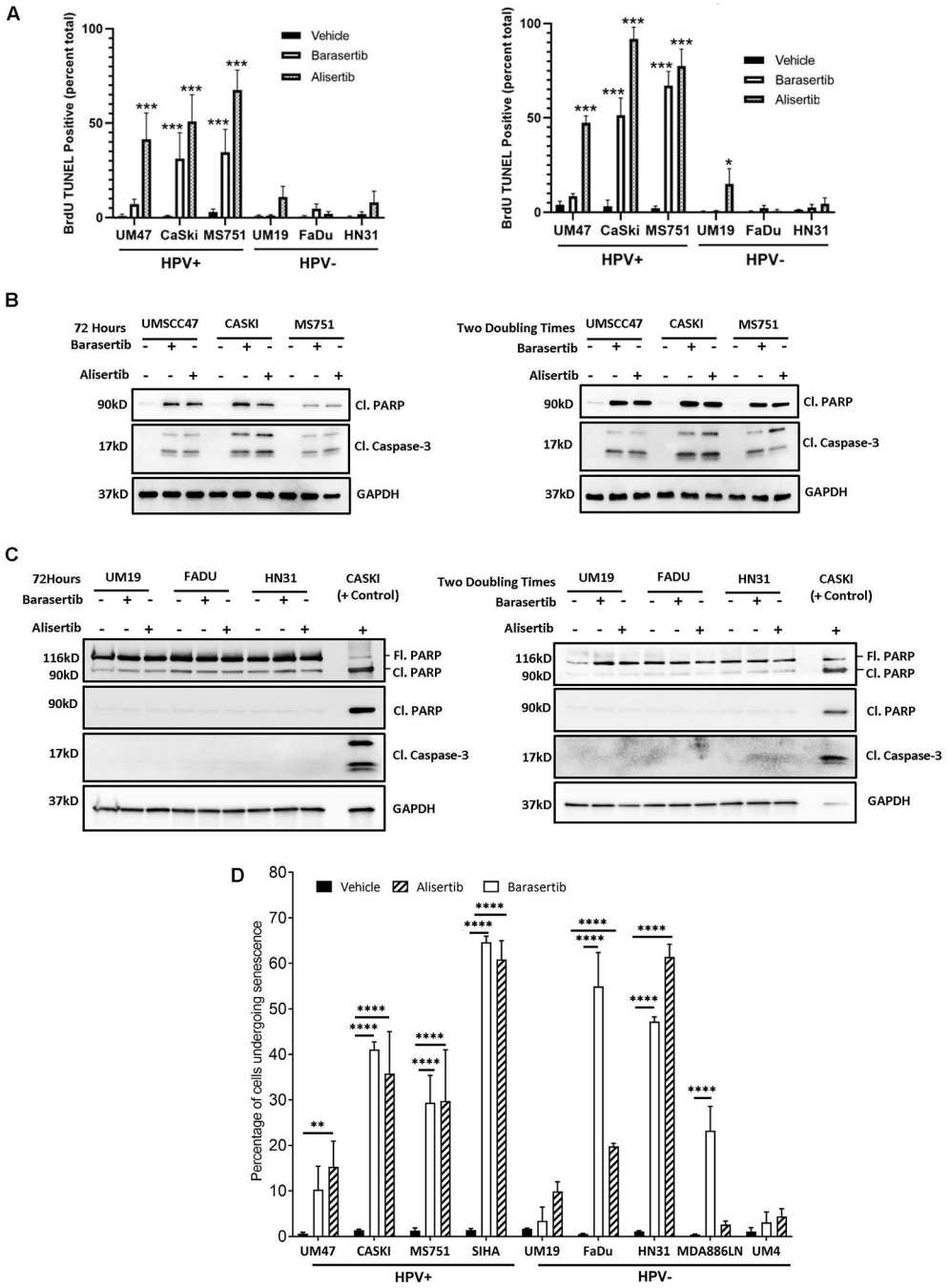


**Figure. 2. Aurora kinase inhibition induces cell death in HPV-positive but not HPV-negative squamous carcinoma cell lines *in vitro*.**

**A,** Bromodeoxyuridine (BrDU)-TUNEL assays were used to measure apoptosis with flow cytometry in 3 HPV-positive and 3 HPV-negative squamous carcinoma cell lines treated with 50 nmol/L barasertib or 200 nmol/L alisertib for 72 hours (left panel) or 2 doubling times (right panel). BrdU positive apoptotic cells were detected and quantified. The bar graph indicates the percentages of apoptotic cells with fragmented DNA in HPV-positive and HPV-negative cell lines. Values are the means ± the standard deviations for 3 independent

experiments. **B-C,** Immunoblots of cleaved PARP (Cl. PARP) and cleaved caspase-3 (Cl. Caspase-3) levels in 3-HPV positive and 3 HPV-negative cell lines after barasertib or alisertib treatment for (**B**) 2 doubling times or (**C**) 72 hours. **D,** We used flow cytometry to detect and quantify senescent cells in 4 HPV-positive and 5 HPV-negative cell lines treated with 50 nmol/L barasertib or 200 nmol/L alisertib for 72 hours. ** $P \leq 0.005$; **** $P \leq 0.0001$ (unpaired, 2-tailed Student *t* test). UM47, UMSCC47; GAPDH, glyceraldehyde 3-phosphate dehydrogenase.

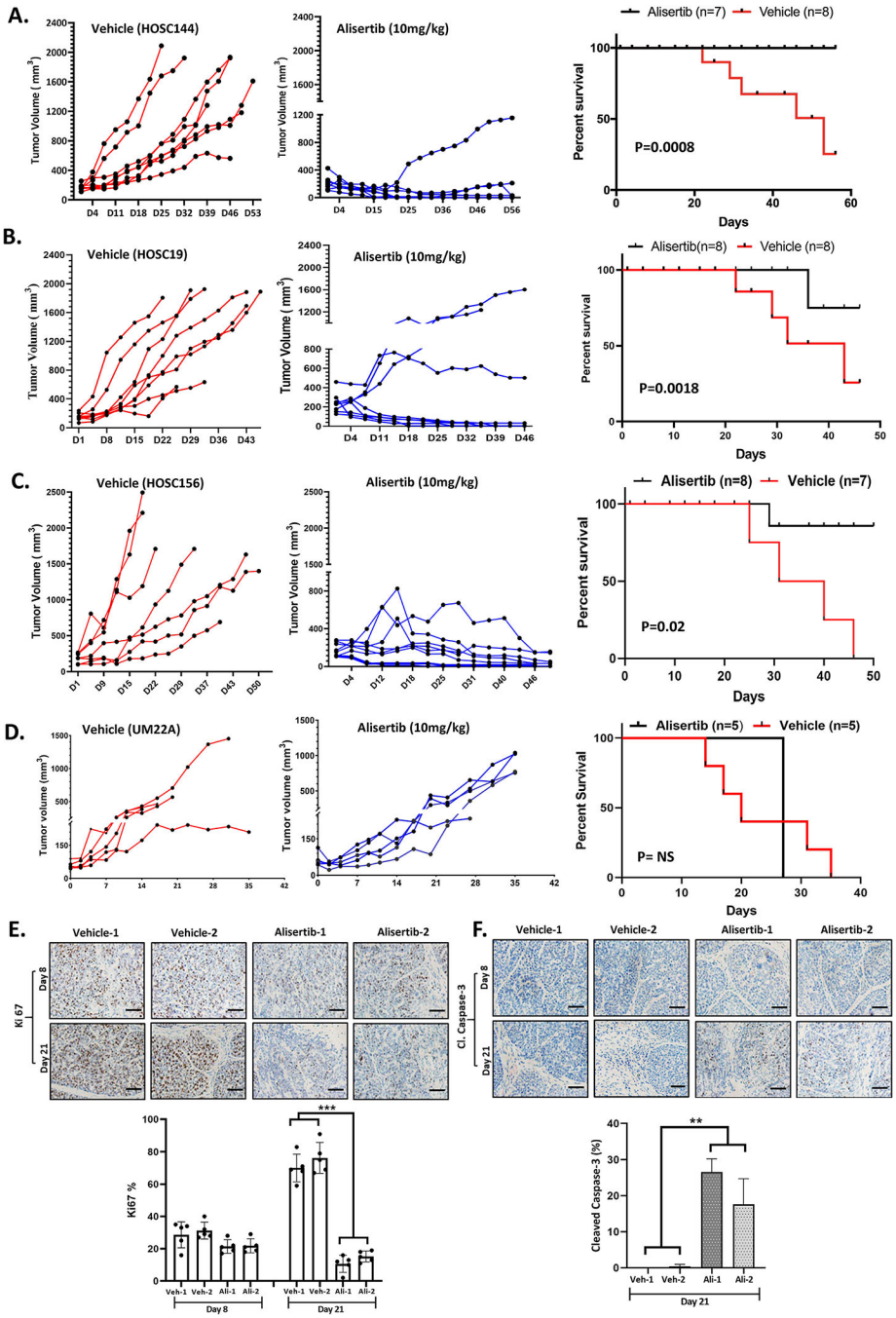


**Figure. 3. Aurora kinase A inhibition leads to tumor regression and apoptosis *in vivo* in HPV-positive PDX models, but not in an HPV-negative cell line.**

PDX tumors (HOSC144 [(**A**), (**E**), and (**F**)], HOSC19 (**B**) and HOSC156 (**C**)] were implanted into the flanks of nude mice. After engraftment, mice were randomized and assigned into 1 of 2 treatment groups: vehicle (β-cyclodextrin, $n = 8$) or alisertib (10 mg/kg, $n = 8$). Mice were treated for 3 weeks by daily oral gavage. Tumor size was measured twice a week. **A-C**. *In vivo* tumor growth curves for individual mice (left 3 panels). Survival (right panels) was measured using the Kaplan-Meier method (20). **D**. HPV-negative UMSCC22A

cells were injected subcutaneously ($3 \times 10^6$ cells) on the right flanks of the mice. Once the tumor volume reached ≥60 $mm^3$, mice were randomized into treatment groups. Mice were treated with vehicle or 10 mg/kg alisertib by oral gavage for 5 days per week for 21 days. Tumor size was measured twice a week. **E-F,** Immunohistochemical staining for (**E**) cleaved Ki67 (upper left panel) with quantification of proliferative cells by Ki-67 (bottom left panel). The Ki67 (%) was calculated as the ratio of proliferative cells to total cells in each field, using five random fields and (**F**) cleaved caspase-3 (Cl. Caspase-3; upper right panel) with quantification of apoptotic cells by staining Cl caspase-3 (lower right panel). The apoptotic (%) was calculated as the ratio of apoptotic cells to total cells in each field, using five random fields in HOSC144 PDX tumors after 8 or 21 days of treatment with either vehicle or alisertib. ** $P \leq 0.01$; *** $P \leq 0.001$. Bars, 100 μM.

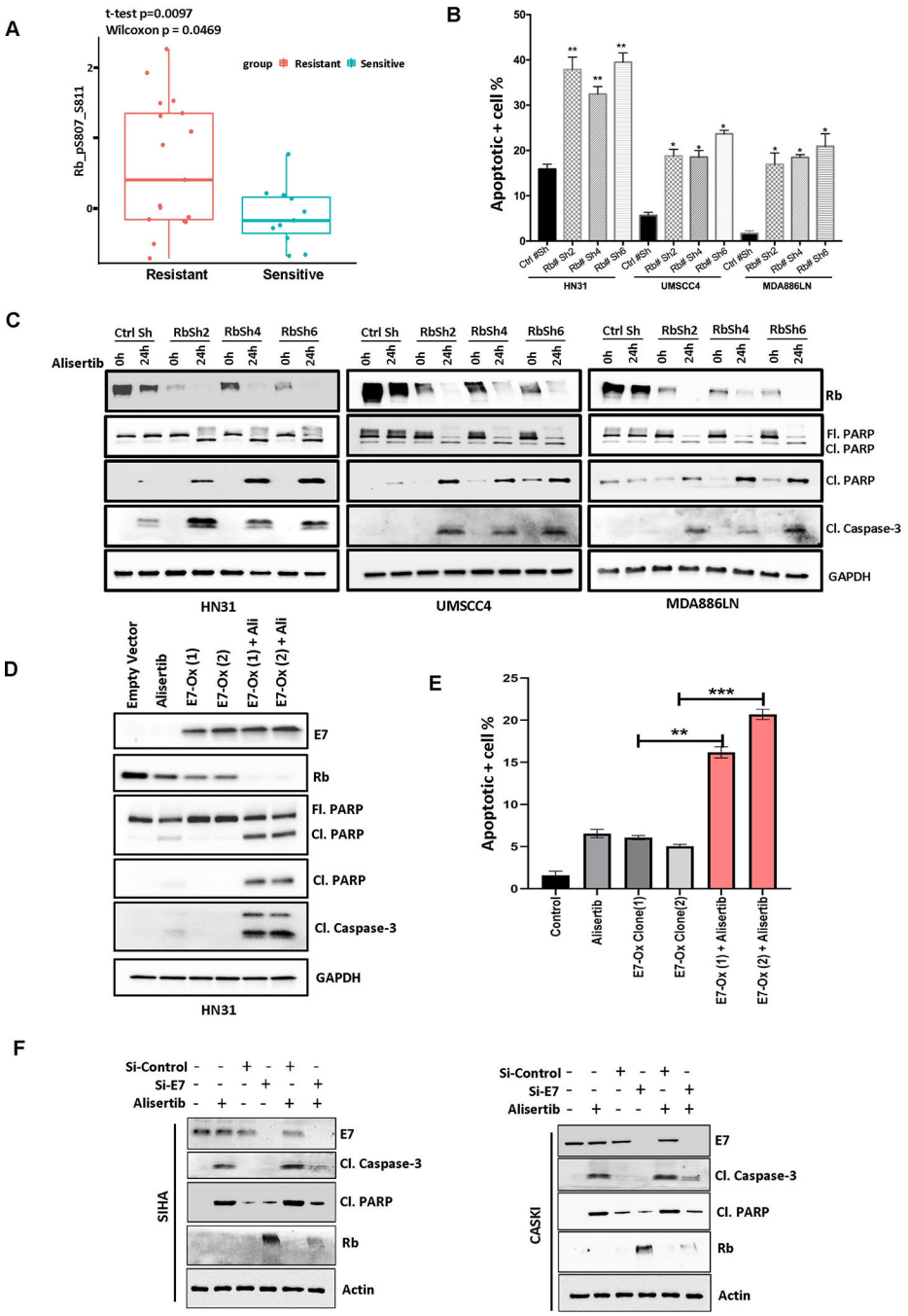


**Figure. 4. Effect of Rb expression on Aurora kinase A inhibition–induced apoptosis.**

**A**, Levels of pRb (S807/S811) protein expression in alisertib-sensitive and -resistant squamous cancer cell lines as defined by AOC_LD values. Each data point represents 1 cell line. Box plots show the median pRb (S807/S811) levels and 95% confidence intervals across all cell lines in the category. *t*-test $P = 0.0097$. **B,** HPV-negative HNSCC cells (HN31, UMSCC4, and MDA886LN) were infected with distinct, lentivirus-based shRNAs (Sh2, Sh4, and Sh6) to stably knock down the expression of *RB1* or were treated with control (Ctrl) shRNA. Cells were then treated with 300 nmol/L alisertib for 24 hours before annexin

V-PE/7AAD staining and analysis with flow cytometry. The bar graph represents the ratio of apoptosis (late plus early) among different groups. Values are the means ± the standard deviations for 3 independent experiments. *$P$ <0.05; **$P$ <0.005; unpaired, 2-tailed Student $t$-test. **C**, Cells from B were treated with 300 nmol/L alisertib for 24 hours before lysis and immunoblotting with the indicated antibodies. **D-E,** HN31 cells were stably transfected with an E7 plasmid and treated with 300 nmol/L alisertib for 24 hours before lysis and immunoblotting with **(D)** the indicated antibodies or (**E**) annexin-PE staining to measure apoptosis. Values are the means ± the standard deviations for 3 independent experiments. ** $P \leq 0.01$; *** $P \leq 0.001$. **F,** Two HPV-positive cell lines were transfected with 10 nmol/L siRNA oligonucleotides specific to E7 or with control oligonucleotides. Twenty-four hours later, the cells were treated with 300 nmol/L alisertib for an additional 24 hours and then harvested and immunoblotted for the indicated proteins. Representative results from 3 independent experiments are shown. Cl, cleaved; Fl, full length; GAPDH, glyceraldehyde 3-phosphate dehydrogenase; Ox, overexpression.

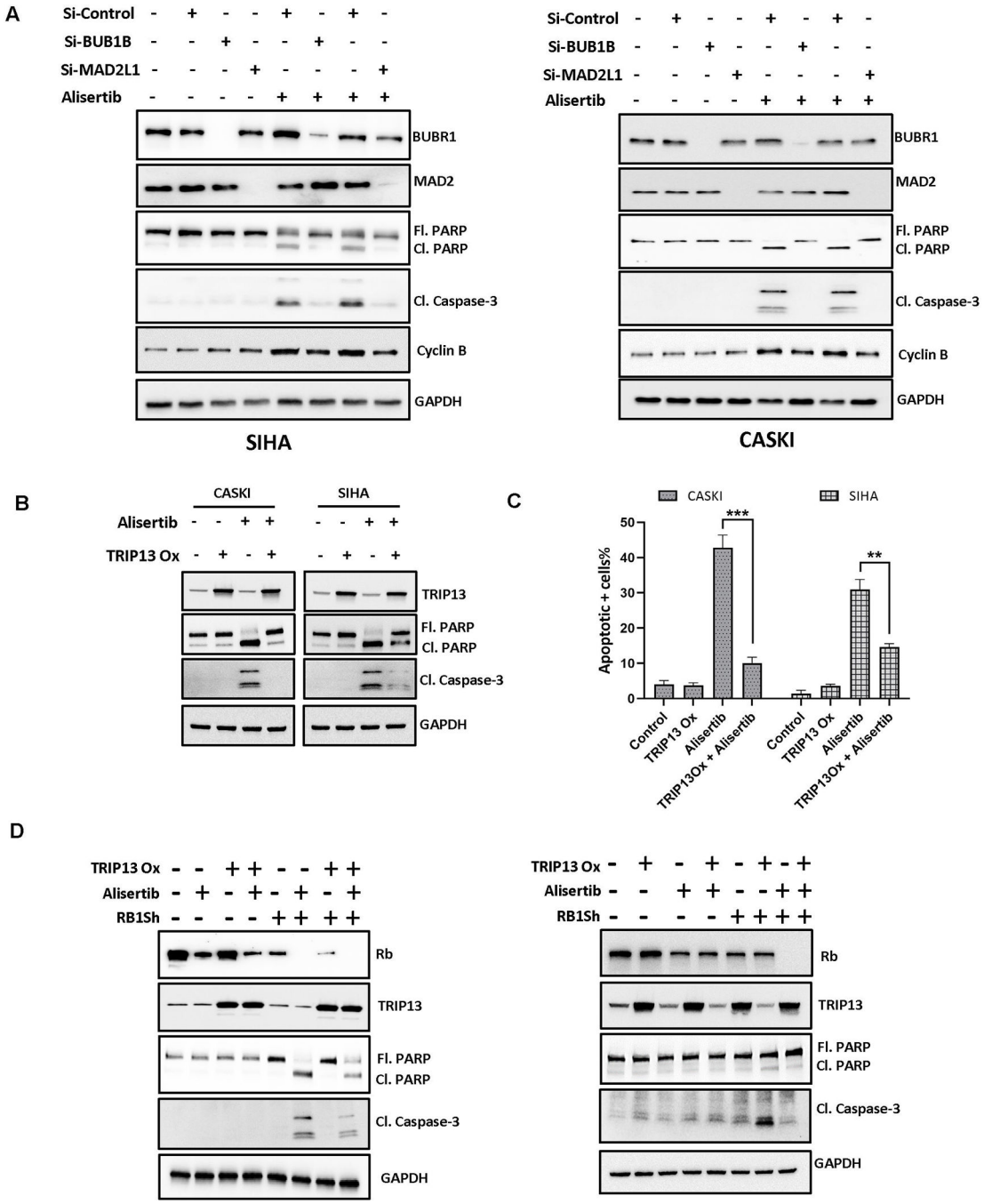


**Figure. 5. The alteration of mitotic checkpoint proteins rescues Rb-depleted cells from Aurora kinase inhibitor–induced apoptosis.**

**A,** Two HPV-positive cell lines (CASKI and SIHA) were transfected with *BUB1B* or *MAD2L1* siRNA and then treated for 24 hours with 300 nmol/L alisertib before lysis and immunoblotting with the indicated antibodies. **B,** TRIP13 was transiently overexpressed (Ox) in 2 HPV-positive cell lines that were treated for 24 hours with 300 nmol/L alisertib before lysis and immunoblotting for the indicated proteins. **C,** HPV-positive cell lines with TRIP13 overexpression were treated with 300 nmol/L alisertib for 32 hours and then

stained for annexin V-PE/7AAD staining and analysis with flow cytometry to measure apoptosis. The bar graph represents the ratio of apoptosis (late plus early) among different groups. Values are the means ± the standard deviations for 3 independent experiments. ** $P \leq 0.01$; *** $P \leq 0.001$; unpaired, 2-tailed Student *t*-test. **D**, HN31 (left panel) and MDA886LN (right panel) cells expressing *RB1* or control shRNA were transfected with a plasmid for TRIP13. After 24 hours, cells were treated with 300 nmol/L alisertib and then lysed for immunoblotting. Cl, cleaved; Fl, full length; GAPDH, glyceraldehyde 3-phosphate dehydrogenase.

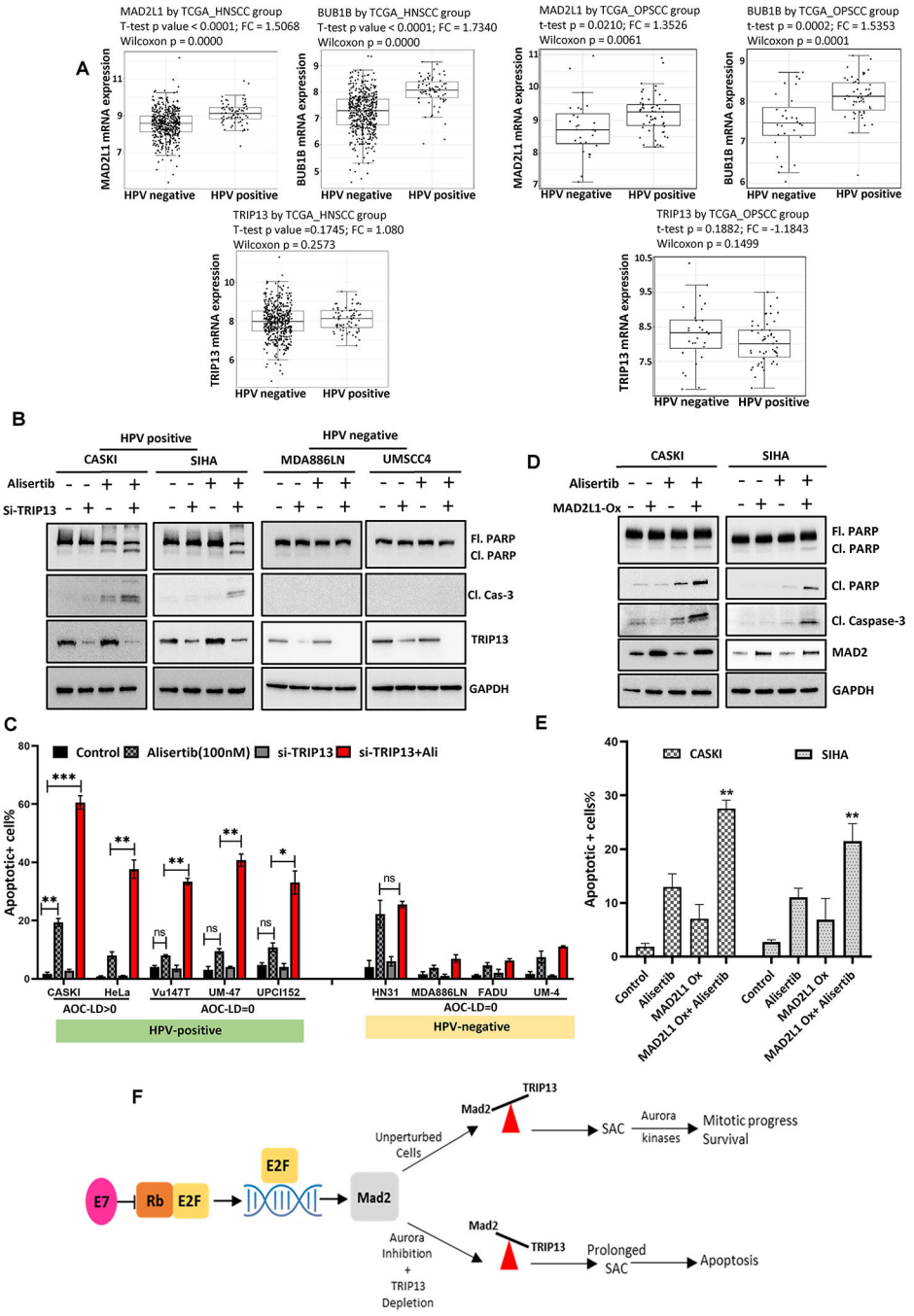


**Figure. 6. Disturbing the balance of TRIP13 and MAD2 enhances Aurora kinase inhibition–induced apoptosis.**

**A,** mRNA expressions of *MAD2L1*, *BUB1B* and *TRIP13* in HNSCC HPV-positive (n = 70) and HPV-negative (n = 447) HNSCC patient tumors from the TCGA (left panel) and in HPV-positive (n=51) and HPV-negative OPSCC [(n=28), right panel]. **B-C,** TRIP13 was depleted by siRNA in HPV-positive and negative cell lines. Cells were then treated with 100 nmol/L alisertib for 36 hours before being subjected to (**B**) lysis and immunoblotting with the indicated antibodies or annexin-PE staining to measure apoptosis using flow cytometry

or (**C**). **D-E,** The *MAD2L1* plasmid was transiently transfected into 2 HPV-positive cell lines that were then treated with 100 nmol/L alisertib for 24 hours before being subjected to (**D**) lysis and immunoblotting for the indicated proteins or (**E**) annexin-PE staining to measure apoptosis. Values are the means ± the standard deviations for 3 independent experiments (** $P \leq 0.01$). Cl, cleaved; Fl, full length; GAPDH, glyceraldehyde 3-phosphate dehydrogenase; Ox, overexpression. **F,** Model of the synthetic lethality between TRIP13 and Aurora kinase A. HPV-positive, Rb deficient cancer cells rely on both TRIP13 and Aurora kinase activity to maintain mitotic fidelity, such that their combined inhibition will lead to a prolonged spindle assembly checkpoint (SAC), irreversible mitotic arrest, and cancer cell death.